Proceedings of the European Conference Physics of Magnetism 2011 (PM'11), Poznań, June 27–July 1, 2011

Investigation of the Magnetization Reversal Process of High-Remanent $Nd_{10}Fe_{83}Zr_1B_6$ Alloy in the As-Cast State

A.E. Ceglarek*, D. Płusa, M.J. Dośpiał, M.G. Nabiałek and P. Pietrusiewicz
Institute of Physics, Częstochowa University of Technology, al. Armii Krajowej 19, 42-200 Częstochowa, Poland

In this work the magnetic properties of ribbons with composition of $Nd_{10}Fe_{83}Zr_1B_6$ obtained by using the melt-spinning method were studied. From the X-ray diffraction patterns the phase composition was determined. It was found that investigated alloy was composed of α-Fe and $Nd_2Fe_{14}B$ phases. From the peaks broadening the grain sizes of α-Fe and $Nd_2Fe_{14}B$ phases were estimated as equal to 20 nm and 40 nm, respectively. From the recoil curves the reversible $\mu_0 M_{\rm rev}$ and irreversible $\mu_0 M_{\rm irr}$ parts of magnetization and differential susceptibility $\chi_{\rm rev}$ and $\chi_{\rm irr}$ were determined as a function of an applied field. From these dependences it was found that the pinning of domain walls at the grain boundaries is the main magnetization reversal process. The interactions between grains were investigated by means of the δM plot. It was stated that short range exchange interaction between grains of hard and soft phases are dominant and causes the remanence enhancement.

PACS: 75.30.Et, 75.50.Vv, 75.50.Ww, 75.60.Ej, 75.60.Jk

1. Introduction

The two-phase nanocomposite magnetic materials consisting of hard $Nd_2Fe_{14}B$ and soft α-Fe or Fe_3B nanoscaled grains have been intensively investigated since the first announcements by Cooehorn et al. [1] and Manaf et al. [2] on the remanence enhancement arising from the exchange interaction between the grains with different magnetic hardness. In such alloys the high anisotropy field of hard $Nd_2Fe_{14}B$ phase is combined with the high saturation magnetization of soft α-Fe or Fe_3B phases. Such nanocomposites are very attractive material for production of permanent magnets (called the exchange spring magnets [3]) due to the possibility to obtain the high remanence and consequently the high maximum energy product $(BH)_{\rm max}$. Unfortunately, the presence of soft magnetic phase results in decrease in coercivity. Therefore the high values of maximum energy product predicted by theory are not achieved up till now in spite of many attempts which have been made to improve the microstructure and thus coercivity.

Exchange coupling between neighbouring grains causing the remanence enhacement above $\mu_0 M_{\rm R} = 0.5\mu_0 M_{\rm S}$ reduces simultaneously the coercivity. It is essential that this reduction should not be smaller than $\mu_0 H_{\rm C} = 0.5\mu_0 M_{\rm R}$ in order to get the appropriately high maximum energy product [3, 4].

The melt spinning method is a simple and economical way to prepare the nanocomposite ribbons from alloys with lower amount of expensive Nd in comparison with the stoichiometric one. The nanocomposites can be obtained either by formation of amorphous alloy by rapid quenching of liquid alloy on rotating cooper wheel and the crystallization by annealing or directly solidifying the melt. The better magnetic properties can be obtained by the latter method because the possibility of grain growth during annealing in a former one [5].

* corresponding author; e-mail: a.ceglarek@go2.pl

The large number of experimental investigation on Nd–Fe–Zr–B type compounds have been performed up to now. These articles usually describe the manufacturing conditions and their influence on structure, magnetic properties and thermal stability [6–9]. But none of them were devoted to magnetization reversal processes in $Nd_{10}Fe_{83}Zr_1B_6$ ribbons.

The aim of this paper was to obtain the exchange coupled nanocomposite ribbons having the good magnetic properties in an as-cast state and discuss the coercivity mechanism in that sample.

2. Material and experimental methods

In this work, the nanocomposites were obtained on the base of $Nd_2Fe_{14}B$ alloy. The ingots of the alloy were obtained by arc-melting method in the protective argon atmosphere using high purity constituents. Boron was added in the form of an alloy with known composition of Fe-45.4 at.%, B-54.6 at.%. Due to the high ability to oxidize the rare earth, titanium was used as an oxygen absorbent. Small amount of Zr was added in order to hinder the grain growth [6].

The nanocomposite ribbons were prepared by rapid quenching of the liquid alloy on a rotating copper wheel with the linear velocity of $20\frac{\rm m}{\rm s}$ and pressure inside of chamber of 0.4×10^5 Pa. The phase composition was determined using Bruker D8 Advance X-ray diffractometer equiped with Lynx Eye semiconductor counter and Cu K_α a radiation source. The average grain sizes were determined using the Sherrer formula.

The hysteresis and recoil loops measurements were performed by the LakeShore vibration sample magnetometer working at magnetic field up to 2 T in room temperature. From the major hysteresis loop measurements the magnetic parameters i.e.: coercivity $\mu_0 H_{\rm C}$, remanence $\mu_0 M_{\rm R}$, saturation magnetization $\mu_0 M_{\rm S}$, and maximum energy product $(BH)_{\rm max}$ were determined. From the recoil curves measured in both magnetization and demagnetization directions the reversible $\mu_0 M_{\rm rev}$ and irreversible $\mu_0 M_{\rm irr}$ magnetization and differential suscepti-

bility $\chi_{\rm rev}$ and $\chi_{\rm irr}$ components were determined. The $\mu_0 M_{\rm irr}^{\rm r}$ is the value of the magnetization when the magnetizing field is reduced to zero along the recoil curve, $\mu_0 M_{\rm irr}^{\rm d}$ is the magnetization when the reversed field applied to previously saturated sample is reduced to zero. The $\mu_0 M_{\rm rev}^{\rm (r,d)}$ is defined as [10]:

$$\mu_0 M_{\rm rev}^{\rm (r,d)} = \mu_0 M - \mu_0 M_{\rm irr}^{\rm (r,d)}. \quad (1)$$

The interaction between grains were investigated using the δM plot [11]:

$$\delta M = \frac{\mu_0 M_{\rm irr}^{\rm d}}{\mu_0 M_{\rm R}} - \left(1 - 2\frac{\mu_0 M_{\rm irr}^{\rm r}}{\mu_0 M_{\rm R}}\right), \quad (2)$$

where $\mu_0 M_{\rm R}$ is the remanence.

All magnetic measurements were performed for ribbons, whose thickness and width is equal to 2 mm and 1 mm, respectively.

3. Results and discussion

From the qualitative analysis of X-ray pattern it was found that the investigated alloy is composed of two phases which includes magnetically hard $Nd_2Fe_{14}B$ and α-Fe soft phases. Using the Sherrer formula the average grain sizes of both phases were estimated as equal to (27 ± 3) nm, (9 ± 1) nm, respecively.

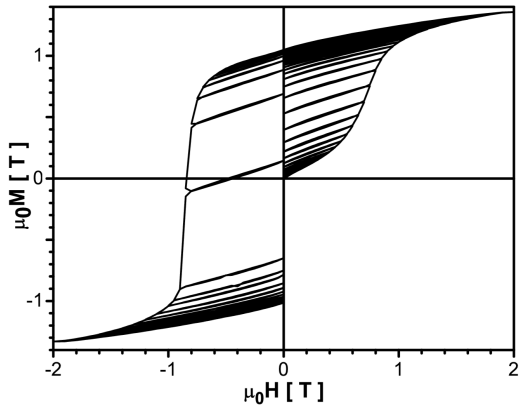

Fig. 1. Major and recoil loops measurement in magnetization and demagnetization.

In Fig. 1 the recoil curves with major hysteresis loop are presented. The magnetic parameters determined from the major loop are as follows: $\mu_0 H_{\rm C} = 0.84$ T, $\mu_0 M_{\rm R} = 1.05$ T, $\mu_0 M_{\rm S} = 1.36$ T and $(BH)_{\rm max} = 160\ \frac{\rm kJ}{\rm m^3}$. The hysteresis loop of the ribbons investigated is smooth showing single phase behaviour and a good rectangularity and has a high remanence ratio of $\frac{M_{\rm R}}{M_{\rm S}} = 0.77$. Such a shape is typical for single or multi-phase material with strong exchange interaction.

The investigated ribbon belongs to high-remanent exchange coupled type of alloys having $\frac{M_{\rm R}}{M_{\rm S}} > 0.5$ [12]. The increased value of remanence results from strong exchange interactions between grains of magnetically soft and hard phases. The ribbons obtained in this work exhibit quite high coercivity fulfilling the condition $\mu_0 H_{\rm C} > 0.5\mu_0 M_{\rm R}$ needed for obtaining the high maximum energy product.

As it is seen in Fig. 1 the recoil curves for the investigated ribbon are not completely reversible and enclose some areas but they are much smaller than that published for similar samples [13] suggesting the existence of stronger intergrain coupling.

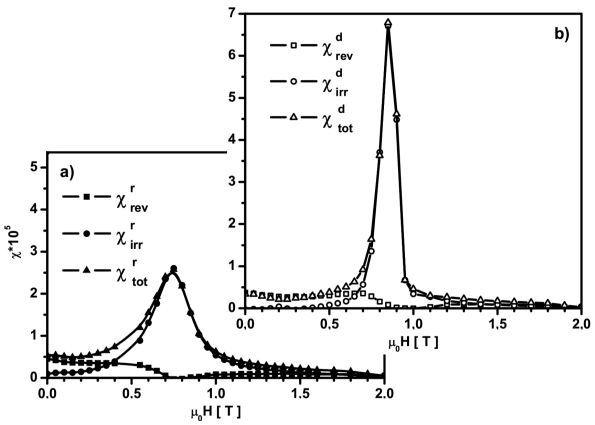

Fig. 2. Field dependence of the total magnetization, reversible and irreversible components of total magnetization during (a) the initial magnetization, (b) the demagnetization.

Field dependence of reversible and irreversible magnetization components for both polarization directions of magnetization is shown in Fig. 2a,b. For comparison the reversible and irreversible magnetization in the second quadrant of hysteresis loop were calculated as

$$\mu_0 M_{\rm rev} = -\mu_0 M_{\rm rev}^{\rm d},$$
$$\mu_0 M_{\rm irr} = \frac{(\mu_0 M^{\rm d} - \mu_0 M_{\rm irr}^{\rm d})}{2}. \quad (3)$$

The dependences of reversible magnetization component as a function of an applied field in both polarization directions are similar. Its changes are associated with a reversible rotation of magnetization vector in magnetically soft iron grains and magnetically hard $Nd_2Fe_{14}B$ grains. Small peaks are observed at an applied magnetic field lower than the coercivity of the sample. Its presence may be associated with α-Fe and $Nd_2Fe_{14}B$ grains decoupling.

The dependences of irreversible magnetization component are characteristic for materials in which the main demagnetization mechanism is the pinning of domain walls at the grain boundaries [14]. At an applied magnetizing (or demagnetizing) field lower than the sample coercivity the irreversible magnetization components have the small values (or close to zero). At higher fields the irreversible components of magnetization rise rapidly and exceed the reversible ones.

The changes in magnetization are better seen in a field dependence of differential susceptibilities for both field directions presented in Fig. 3a,b.

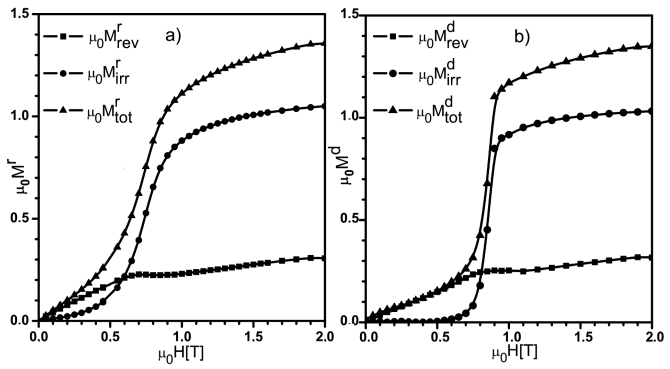

Fig. 3. The reversible and irreversible susceptibilities components measured in the direction of magnetization (a) and demagnetization (b).

The irreversible susceptibility curves the peaks at external magnetic field close to the coercivity of sample indicating that the main magnetization reversal mechanism is the pinning of domain walls [15]. Narrow and high peak in the demagnetizing direction means that the distribution of grain sizes is also narrow and microstructure is homogeneous. Parameters like peaks location and full width at half maximum of magnetic susceptibility are not the same and the high peaks do not fulfill condition resulting from Stoner–Wohlfarth theory for non-interacting uniaxial single-domain articles [11]:

$$2 \cdot \chi^{\mathrm{r}}_{\mathrm{irr,max}} = \chi^{\mathrm{d}}_{\mathrm{irr,max}}. \tag{4}$$

Such results confirm the presence of interactions between grains.

The presence of strong interaction between the grains of both phases was also confirmed by the δM (Eq. (1)) plot seen in Fig. 4. According to Wohlfarth theory δM is equal to zero for noninteracting uniaxial single-domain particles. The δM is such relation and is not equal to zero which is not valid for the sample investigated.

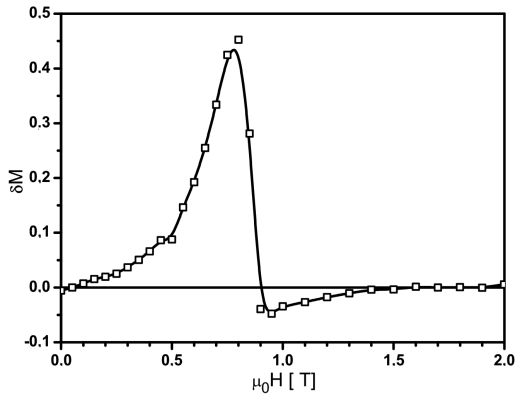

Fig. 4. Differential susceptibility curves of the sample.

At a field lower than the sample coercivity (< 0.9 T) the $\delta M(H)$ value is positive and at higher fields changes its sign [16]. Such shape of the $\delta M(H)$ plot is characteristic for materials in which the short-range exchange interaction dominates over the magnetostatic one and supports the magnetization process.

4. Concluding remarks

The nanocomposite $Nd_{10}Fe_{83}Zr_1B_6$ ribbon is composed of strongly exchange coupled α-Fe and $Nd_2Fe_{14}B$ grains. Manufactured ribbons in as-cast state have better magnetic properties (i.e. $(BH)_{\max} = 160$ $\frac{\mathrm{kJ}}{\mathrm{m}^3}$ and $\mu_0 M_{\mathrm{R}} = 1.05$ T) in comparison to annealed ribbons with similar composition founded in the literature (i.e. $(BH)_{\max} = 140$ $\frac{\mathrm{kJ}}{\mathrm{m}^3}$ and $\mu_0 M_{\mathrm{R}} = 0.95$ T [7]). The coercivity equal to 0.87 T fulfills the condition $\mu_0 H_{\mathrm{C}} > 0.5 \mu_0 M_{\mathrm{R}}$. The existing of exchange interaction confirmed by positive δM is the source of the remanence and $(BH)_{\max}$ enhancement. High value of coercivity results from the small grain sizes (27 nm and 9 nm for α-Fe and $Nd_2Fe_{14}B$ phases, respectively). The main mechanism of the magnetization reversal is the pinning of domain walls.

References

[1] R. Coehoorn, D.B. Mooji, C. DeWaard, *J. Magn. Magn. Mater.* **80**, 101 (1989).

[2] A. Manaf, R.A. Buckley, H.A. Davies, *J. Magn. Magn. Mater.* **128**, 302 (1993).

[3] E.F. Kneller, R. Hawig, *IEEE Trans. Magn.* **27**, 3588 (1991).

[4] H. Kronmüller, D. Goll, *Scr. Mater* **47**, 551 (2002).

[5] Z. Tian, S. Li, K. Peng, B. Gu, J. Zhang, M. Lu, Y. Du, *Mater. Sci. Eng. A* **380**, 143 (2004).

[6] C. Wang, M. Yan, Q. Li, *Mater. Sci. Eng. B* **150**, 77 (2008).

[7] C. Wang, M. Yan, *Mater. Sci. Eng. B* **128**, 216 (2006).

[8] S. Li, B. Gu, H. Bi, Z. Tian, G. Xie, Y. Zhu, Y. Du, *J. Appl. Phys.* **92**, 7514 (2002).

[9] H. Sheng, X. Zeng, D. Fu, F. Deng, *Physica B* **405**, 690 (2010).

[10] D.C. Crew, S.H. Farrant, P.G. McCormick, R. Street, *J. Magn. Magn. Mater.* **163**, 299 (1996).

[11] E.P. Wohlfarth, *J. Appl. Phys.* **29**, 595 (1958).

[12] E.C. Stoner, W.P. Wohlfarth, *Philos. Trans. R. Soc. Lond. A* **240**, 599 (1948).

[13] Ch. Rong, Y. Lium, P. Liu, *Appl. Phys. Lett.* **93**, 042508 (2008).

[14] C.G. Hadjipanayis, A. Kim, *J. Appl. Phys.* **63**, 3310 (1988).

[15] M. Dospial, M. Nabiałek, M. Szota, D. Płusa, *J. Alloys Comp.*, 2011, doi:10.1016/j.jallcom.2010.12.043.

[16] Y. Sen, S. Xiaoping, D. Youwei, *Microelectron. Eng.* **66**, 121 (2003).